

Spectral co-Clustering in Rank-deficient Multi-layer Stochastic co-Block Models

Wenqing Su¹, Xiao Guo², Xiangyu Chang³, and Ying Yang¹

¹Department of Mathematical Sciences, Tsinghua University

²School of Mathematics, Northwest University

³School of Management, Xi'an Jiaotong University

Abstract

Modern network analysis often involves multi-layer network data in which the nodes are aligned, and the edges on each layer represent one of the multiple relations among the nodes. Current literature on multi-layer network data is mostly limited to undirected relations. However, direct relations are more common and may introduce extra information. In this paper, we study the community detection (or clustering) in multi-layer directed networks. To take into account the asymmetry, we develop a novel spectral-co-clustering-based algorithm to detect *co-clusters*, which capture the sending patterns and receiving patterns of nodes, respectively. Specifically, we compute the eigen-decomposition of the *debiased* sum of Gram matrices over the layer-wise adjacency matrices, followed by the k -means, where the sum of Gram matrices is used to avoid possible cancellation of clusters caused by direct summation. We provide theoretical analysis of the algorithm under the multi-layer stochastic co-block model, where we relax the common assumption that the cluster number is coupled with the rank of the model. After a systematic analysis of the eigen-vectors of population version algorithm, we derive the misclassification rates which show that multi-layers would bring benefit to the clustering performance. The experimental results of simulated data corroborate the theoretical predictions, and the analysis of a real-world trade network dataset provides interpretable results.

Keywords: Multi-layer directed networks, Co-clustering, Spectral methods, Bias-correction

1 Introduction

Multi-layer network data arise naturally among various domains, where the nodes are the entities of interest and each network layer represents one of the multiple relations of the same set of entities (Mucha et al., 2010; Holme and Saramäki, 2012; Kivelä et al., 2014; Boccaletti et al., 2014). For example, the gene co-expression multi-layer network consists of genes co-expressed at different developmental stages of the animal, and the gene expression patterns at different stages may differ yet remain highly correlated (Bakken et al., 2016; Zhang and Cao, 2017). The above example involves undirected relations. In real-world networks, more common relations are *directed*. For example, the Worldwide Food and Agricultural Trade (WFAT) multi-layer network consists of the direct trade relationships among the same set of countries across different commodities. Trade relationships concerning different commodities differ but are not entirely unrelated (De Domenico et al., 2015).

The multi-layer network has received considerable attention recently, see, e.g., Della Rossa et al. (2020); MacDonald et al. (2022); Huang et al. (2022) and references therein. Of particular interest is the community detection or clustering problem, where the goal is to partition the network nodes into disjoint *communities* or *clusters* with the help of multiple layers. We focus on the case that the underlying communities are consistent among all the layers. The community detection of multi-layer networks has been well-studied in the lens of multi-layer stochastic block models (multi-layer SBMs) (Han et al., 2015; Valles-Catala et al., 2016; Paul and Chen, 2016), namely, equipping each layer of the multi-layer network with a stochastic block model (SBM) (Holland et al., 1983). In an SBM, nodes are first partitioned into disjoint communities, and based on the community membership, the nodes are linked with probability specified by a *link probability matrix*. Specifically, Han et al. (2015) studied the asymptotic properties of spectral clustering and maximum likelihood estimation for multi-layer SBMs as the number of layers increases and the number of nodes remains fixed. Paul and Chen (2020) studied several spectral and matrix factorization based methods and provided theoretical guarantees under multi-layer SBMs. Lei et al. (2020)

derived consistent results for a least squares estimation of community memberships and proved consistency of the global optima for general block structures without imposing the positive-semidefinite assumption for individual layers. [Lei and Lin \(2022\)](#) proposed a bias-adjusted spectral clustering for multi-layer SBMs and derived a novel aggregation strategy to avoid the community cancellation of different layers. Considering that different layers may have different community structures, [Jing et al. \(2021\)](#) introduced a mixture multi-layer SBM and proposed a tensor-based method to reveal both memberships of layers and memberships of nodes. Also see [Bhattacharyya and Chatterjee \(2018\)](#); [Pensky and Zhang \(2019\)](#); [Arroyo et al. \(2021\)](#); [Noroozi and Pensky \(2022\)](#) for other recent work.

Despite the great efforts on the community detection of multi-layer networks, the following two issues remain to be tackled. First, existing literature is mostly limited to undirected networks. For directed networks, the most common approach is to simply ignore edge directions and take use of the methods developed for multi-layer undirected networks. However, this simplistic technique is unsatisfactory since the potentially useful information contained in edge directions is not retained. For example, in the WFAT multi-layer network, the trade transactions among countries include both import and export, which is quite different for even a single country. Therefore, clustering nodes regardless of their edge directions would be coarse. To incorporate the asymmetry of directed networks, instead of partitioning the nodes into one set of clusters, it is more reasonable to *co-clustering* the network nodes ([Malliaros and Vazirgiannis, 2013](#); [Rohe et al., 2016](#); [Zhang et al., 2022](#)). That is, clustering the nodes in two ways to obtain *co-clusters*, namely, the row clusters (or the sending clusters) and the column clusters (or the receiving clusters). The nodes in the same row (column) cluster have similar sending (receiving) patterns. Hence, the community detection of multi-layer directed networks should be in the context of co-clustering.

Second, most existing literature on SBMs assumes that the population matrix has rank coupled with the number of underlying communities. That is, the link probability matrix is assumed to be of *full* rank. Such assumption brings benefits to the algebraic properties of the matrices arising from SBMs. However, this assumption is not necessarily met by practical tasks. In the context of multi-layer SBMs, this assumption is inherited in that the population matrix, for example, the *sum* of each layer-wise SBM, is commonly assumed to be of rank

equaling the number of communities, although each *layer-wise* SBM not necessarily satisfies the assumption (Paul and Chen, 2020). Thus, to meet the practical need, it is desirable to study the theoretical properties of the population model of multi-layer directed networks in the rank-deficient regime.

Motivated by the above problems, we study the problem of co-clustering the multi-layer directed network. We typically assume that each layer of network is generated from a stochastic co-block model (ScBM) (Rohe et al., 2016), where the underlying row clusters and column clusters are not necessarily the same. Following convention, we call the model over all layers the *multi-layer* ScBM. The first contribution of this paper is a neat, flexible, and computationally efficient spectral-clustering-based algorithm for co-clustering the multi-layer directed network. To avoid possible cancellation of clusters among layers, we use the *sum of Gram* (SoG) matrices of the row (column) spaces of the layer-wise adjacency matrices as the algorithm’s target matrix in order to detect row (column) clusters. Then, we perform a bias-correction on the two-way SoG matrices to remove the bias that comes from their diagonal entries. After that, we apply the spectral clustering to the two debiased SoG matrices with possibly different cluster numbers. As the leading eigenvectors approximate the row and column spaces of the two debiased SoG matrices, respectively, it is expected that the resulting two sets of clusters contain nodes with similar sending and receiving patterns, respectively. To the best of our knowledge, this is the first work to study the community detection problem for multi-layer directed networks.

The second contribution of this work is that we systematically study the algebraic properties of the population version of SoG matrices whose link probability matrix is *not* necessarily of full rank. In particular, we provide interpretable conditions under which the eigen-decomposition (i.e., the first step of the spectral clustering) of the population version of SoG matrices would reveal the underlying communities in multi-layer ScBMs. Based on these findings, we provide rigorous analysis of the consistency of the community estimates. Specifically, we use the decoupling techniques (de la Peña and Montgomery-Smith, 1995; Lei and Lin, 2022) to derive the concentration inequalities of the sum of quadratic asymmetric matrices. We use the derived inequalities to bound the misclassification rate of the row and column clusters, respectively.

The remainder of the paper is organized as follows. Section 2 presents the model for multi-layer directed networks and investigates its algebraic properties. Section 3 develops the debiased spectral co-clustering algorithm and proves its consistency. Section 4 illustrates the finite sample performance of the proposed method via simulations. Section 5 includes a real-world application of the proposed method to the WFAT dataset. Section 6 concludes the paper and provides possible extensions. Technical proofs are included in the Appendix.

2 The multi-layer ScBM and its algebraic properties

In this section, we first present the multi-layer ScBM for modeling the multi-layer directed network. Next, we study its algebraic properties for understanding the population-wise clustering behavior of spectral co-clustering based on the SoG matrices.

Notes and notation: We use $[n]$ to denote the set $\{1, \dots, n\}$. For a matrix $M \in \mathbb{R}^{m \times n}$ and index sets $I \subseteq [m]$ and $J \subseteq [n]$, M_{I*} and $M_{*,J}$ denote the submatrices of M corresponding to the given rows and columns, respectively. $\|M\|_F$, $\|M\|_{\max}$, $\|M\|_{1,\infty}$, and $\|M\|_{2,\infty}$ denote the Frobenius norm, the element-wise maximum absolute value, the maximum row-wise l_1 norm and the maximum row-wise l_2 norm of a given matrix M , respectively. In addition, $\|\cdot\|_2$ denotes the Euclidean norm of a vector or the spectral norm of a matrix. We will use c, c_0, c_1 and more generally c_i , to denote constant numbers, which will be different from place to place. Following convention, we will use clusters and communities exchangeably.

2.1 Multi-layer ScBMs

Consider the multi-layer directed network with L -layers and n common nodes, whose adjacency matrices are denoted by A_l , where $A_l \in \{0, 1\}^{n \times n}$ for all $1 \leq l \leq L$. We assume that all the layers share common row and column clusters but with possibly different edge densities. In particular, suppose that n nodes are assigned to K_y non-overlapping row clusters and K_z non-overlapping column clusters, respectively. The number of nodes in the row (column) cluster $k \in [K_y]$ ($k \in [K_z]$) is denoted by n_k^y (n_k^z). For $i \in [n]$, the row (column) cluster assignment of node i is given by $g_i^y \in [K_y]$ ($g_i^z \in [K_z]$). Given the cluster assignment, we assume the layer-wise networks are generated independently from the following ScBM (Rohe

et al., 2016). That is, for any pair of nodes $i \neq j$ (with $j \in [n]$) and any layer $l \in [L]$, each $A_{l,ij}$ is generated independently according to

$$A_{l,ij} \sim \text{Bernoulli}(\rho B_{l,g_i^y g_j^z}), \quad (1)$$

where $\rho \in (0, 1]$ is an overall edge density parameter, $B_l \in [0, 1]^{K_y \times K_z}$ denotes the *heterogeneous* link probability matrix indicating the community-wise edge probabilities in each l . While for any $l \in [L]$ and any $i = j$, $A_{l,ii} = 0$. It can be seen from (1) that nodes in a common row (column) cluster are stochastically equivalent senders (receivers) in the sense that they send out (receive) an edge to a third node with equal probabilities. Putting together the L layer-wise networks $\{A_l\}_{l=1}^L$, we say that the multi-layer network is generated from the multi-layer ScBM.

Throughout this paper, we assume that the number of communities is fixed and the community sizes are balanced. Specifically, we make the following Assumption 1.

Assumption 1. *Both the number of row clusters K_y and the number of column clusters K_z are fixed. The community sizes are balanced, that is, there exists a constant $c_0 > 1$ such that each row cluster size is in $[c_0^{-1}n/K_y, c_0n/K_y]$ and each column cluster size is in $[c_0^{-1}n/K_z, c_0n/K_z]$.*

2.2 Algebraic properties of multi-layer ScBMs

It is essential to investigate the algebraic properties of multi-layer ScBMs in order to understand the rationality of a clustering algorithm from the angle of population. Before that, we must specify the clustering algorithm.

For the single-layer ScBM, *spectral co-clustering* (Rohe et al., 2016; Guo et al., 2020) is a popular and effective algorithm, which first computes the singular value decomposition (SVD) of a matrix, say the adjacency matrix A , and then implements k -means on the left and right singular vectors to obtain the row and column clusters, respectively. For the multi-layer ScBM, we also proceed to develop the spectral co-clustering based method to detect the co-clusters. It is natural to use the summation matrix $\sum_{l=1}^L A_l$ as the input of spectral co-clustering. However, such direct summation may lead to cancellation of clusters. For

example, summing up $B_1 := [a, b; c, d]$ and $B_2 := [b, a; d, c]$ would not produce any sensible information for column clusters. Motivated by [Lei and Lin \(2022\)](#), we proceed to use the leading eigenvectors of SoG matrices $\sum_{l=1}^L A_l A_l^T$ and $\sum_{l=1}^L A_l^T A_l$ as the input of subsequent k -means clustering, in order to obtain row and column clusters, respectively, though we will modify the algorithm in the next section.

In the sequel, we investigate the theoretical properties of the eigenvectors of the population version of $\sum_{l=1}^L A_l A_l^T$ and $\sum_{l=1}^L A_l^T A_l$. Before that, we give some notations. Let $Y \in \{0, 1\}^{n \times K_y}$ and $Z \in \{0, 1\}^{n \times K_z}$ be the row and column membership matrices, respectively, where each row are all 0's except one 1. In particular, $Y_{ig_i^y} = 1$ and $Z_{ig_i^z} = 1$ for each i . For $l \in [L]$, denote $\mathcal{P}_l = \rho Y B_l Z^T \in [0, 1]^{n \times n}$, it is easy to see that \mathcal{P}_l serve as the population matrices for A_l , in the sense that $\mathcal{P}_l - \text{diag}(\mathcal{P}_l) = \mathbb{E}(A_l)$. The subsequent lemmas indicate that the rows of the eigenvectors of $\sum_{l=1}^L \mathcal{P}_l \mathcal{P}_l^T$ and $\sum_{l=1}^L \mathcal{P}_l^T \mathcal{P}_l$ could reveal the true row and column clusters, respectively. The proofs of the lemmas are provided in [Appendix B](#). We begin by considering the row clusters.

Lemma 1. *Consider the multi-layer ScBM parameterized by $(Y_{n \times K_y}, Z_{n \times K_z}, \rho \{B_l\}_{l=1}^L)$. Suppose $\text{rank}(\sum_{l=1}^L B_l B_l^T) = K (K \leq K_y)$. Denote the eigen-decomposition of $\sum_{l=1}^L \mathcal{P}_l \mathcal{P}_l^T$ by $U \Lambda^R U^T$, where U is an $n \times K$ matrix with orthonormal columns and Λ^R is a $K \times K$ diagonal matrix. Denote the eigen-decomposition of $\Delta_y \sum_{l=1}^L B_l \Delta_z^2 B_l^T \Delta_y$ by $Q^R D^R Q^{RT}$, where $\Delta_y := \text{diag}(\sqrt{n_1^y}, \dots, \sqrt{n_{K_y}^y})$ and $\Delta_z := \text{diag}(\sqrt{n_1^z}, \dots, \sqrt{n_{K_z}^z})$. Then we have*

- (a) *If $\sum_{l=1}^L B_l B_l^T$ is of full rank, i.e., $K = K_y$, then $Y_{i*} = Y_{j*}$ if and only if $U_{i*} = U_{j*}$. Otherwise, for any $Y_{i*} \neq Y_{j*}$, we have $\|U_{i*} - U_{j*}\|_2 = \sqrt{n_{g_i^y}^{-1} + n_{g_j^y}^{-1}}$.*
- (b) *If $\sum_{l=1}^L B_l B_l^T$ is rank-deficient, i.e., $K < K_y$, then for $Y_{i*} = Y_{j*}$, we have $U_{i*} = U_{j*}$. Otherwise, if $\Delta_y^{-1} Q^R$ has mutually distinct rows and there exists a deterministic positive sequence $\{\zeta_n\}_{n \geq 1}$ such that*

$$\min_{g_i^y \neq g_j^y} \left\| \frac{Q_{g_i^y}^R}{\sqrt{n_{g_i^y}^y}} - \frac{Q_{g_j^y}^R}{\sqrt{n_{g_j^y}^y}} \right\|_2 \geq \zeta_n, \quad (2)$$

then for any $Y_{i} \neq Y_{j*}$, we have $\|U_{i*} - U_{j*}\|_2 \geq \zeta_n$.*

Remark 1. *Note that in the literature on ScBM, the row cluster number K_y , the column cluster number K_z and the rank K of population matrix are commonly coupled, say, it is*

often assumed that $K = K_y \leq K_z$ or $K = K_z \leq K_y$ (Rohe et al., 2016). We here relax this assumption and make the model more practical.

Lemma 1 shows that when two nodes are in the same row cluster, the corresponding rows of U coincides. Conversely, if the nodes do not belong to the same row cluster, a gap is present between their corresponding rows in U . As we will see, this brings confidence to the success of the spectral co-clustering using the sample version of $\sum_{l=1}^L \mathcal{P}_l \mathcal{P}_l^T$. Note that in the rank-deficient case, we additionally require (2) holds to ensure that two rows of U are separable for nodes with different row clusters.

It is desirable to study the sufficient and interpretable condition to satisfy (2). Define a flattened link probability matrix $B^R := [B_1, \dots, B_L] \in [0, 1]^{K_y \times LK_z}$, where the k th row contains the overall sending pattern of the k th row cluster to each of the column clusters across all layers. The following lemma provides an explicit condition on B^R such that (2) holds.

Lemma 2. *Under the same multi-layer ScBM as in Lemma 1 and Assumption 1, if there exists a deterministic positive sequence $\{\eta_n^r\}_{n \geq 1}$ such that B^R satisfies*

$$\min_{g_i^y \neq g_j^y} L^{-1} \langle B_{g_i^y *}^R, B_{g_i^y *}^R \rangle + L^{-1} \langle B_{g_j^y *}^R, B_{g_j^y *}^R \rangle - 2c_1 L^{-1} \langle B_{g_i^y *}^R, B_{g_j^y *}^R \rangle \geq \eta_n^r. \quad (3)$$

Then (2) holds with $\zeta_n = c_2 \sqrt{\eta_n^r/n}$ for some constants $c_1 > 0$ and $c_2 > 0$.

Lemma 2 is interpretable in that it requires certain difference between any two row pairs in B^R . To see this more clearly, if the column clusters are absolutely balanced, then it turns out that $c_1 = 1$ and the LHS of (3) is equivalent to the Euclidean distance (divided by L) of two different rows of B^R .

Remark 2. *It is worth mentioning that we only requires the overall difference of each row cluster pairs. Hence, some layers with weak cluster signal can borrow the strength from other layers with strong cluster signal, which shows the benefit of combining the layer-wise networks.*

The aforementioned results focus on the row clusters. For the column clusters, we can derive similar results if we study instead $\sum_{l=1}^L \mathcal{P}_l^T \mathcal{P}_l$.

Lemma 3. Under the same multi-layer ScBM as in Lemma 1 and suppose $\text{rank}(\sum_{l=1}^L B_l^T B_l) = K' (K' \leq K_z)$. Denote the eigen-decomposition of $\sum_{l=1}^L \mathcal{P}_l^T \mathcal{P}_l$ by $V \Lambda^C V^T$, where V is an $n \times K'$ matrix with orthonormal columns and Λ^C is a $K' \times K'$ diagonal matrix. Denote the eigen-decomposition of $\Delta_z \sum_{l=1}^L B_l^T \Delta_y^2 B_l \Delta_z$ by $Q^C D^C Q^{CT}$. Then we have

(a) If $\sum_{l=1}^L B_l^T B_l$ is of full rank, i.e., $K' = K_z$, then $Z_{i*} = Z_{j*}$ if and only if $V_{i*} = V_{j*}$. Otherwise, for any $Z_{i*} \neq Z_{j*}$, we have $\|V_{i*} - V_{j*}\|_2 = \sqrt{n_{g_i^z}^{-1} + n_{g_j^z}^{-1}}$.

(b) If $\sum_{l=1}^L B_l^T B_l$ is rank-deficient, i.e., $K' < K_z$, then for $Z_{i*} = Z_{j*}$, we have $V_{i*} = V_{j*}$. Otherwise, if $\Delta_z^{-1} Q^C$ has mutually distinct rows and there exists a deterministic positive sequence $\{\xi_n\}_{n \geq 1}$ such that

$$\min_{g_i^z \neq g_j^z} \left\| \frac{Q_{g_i^z*}^C}{\sqrt{n_{g_i^z}}} - \frac{Q_{g_j^z*}^C}{\sqrt{n_{g_j^z}}} \right\|_2 \geq \xi_n, \quad (4)$$

then for any $Z_{i*} \neq Z_{j*}$, we have $\|V_{i*} - V_{j*}\|_2 \geq \xi_n$.

Lemma 3 shows that the leading eigenvectors of $\sum_{l=1}^L \mathcal{P}_l^T \mathcal{P}_l$ can expose the true underlying column clusters, where when $\sum_{l=1}^L B_l^T B_l$ is rank-deficient, we need extra condition (4). In the following Lemma 4, we provide a sufficient condition under which (4) holds. In particular, when $\sum_{l=1}^L B_l^T B_l$ is rank-deficient, we provide an interpretable condition on the flattened matrix $B^C := [B_1^T, \dots, B_L^T] \in [0, 1]^{K_z \times LK_y}$ which is sufficient for (4).

Lemma 4. Under the same multi-layer ScBM as in Lemma 3 and Assumption 1, if there exists a deterministic positive sequence $\{\eta_n^c\}_{n \geq 1}$ such that B^C satisfies

$$\min_{g_i^z \neq g_j^z} L^{-1} \langle B_{g_i^z*}^C, B_{g_i^z*}^C \rangle + L^{-1} \langle B_{g_j^z*}^C, B_{g_j^z*}^C \rangle - 2c_1 L^{-1} \langle B_{g_i^z*}^C, B_{g_j^z*}^C \rangle \geq \eta_n^c.$$

Then (4) holds with $\xi_n = c_2 \sqrt{\eta_n^c/n}$ for some constants $c_1 > 0$ and $c_2 > 0$.

3 Debiased spectral co-clustering and its consistency

In this section, we formally present the spectral-co-clustering algorithm based on the SoG matrices, where we provide a bias-adjustment strategy to remove the bias of the SoG matrix. Then we study its theoretical properties in terms of misclassification rate.

3.1 Debiased spectral co-clustering

We begin by considering the row clusters. As illustrated in Section 2, we have shown that $\sum_{l=1}^L A_l A_l^T$ is a good surrogate of $\sum_{l=1}^L A_l$ for avoiding possible row clustering cancellation, and we provide theoretical support that the population-wise matrix $\sum_{l=1}^L \mathcal{P}_l \mathcal{P}_l^T$, has eigenvectors that can reveal the true underlying row clusters, where recall that $\mathcal{P}_l - \text{diag}(\mathcal{P}_l) = \mathbb{E}(A_l)$. However, similar to the undirected case studied in [Lei and Lin \(2022\)](#), we will see that $\sum_{l=1}^L A_l A_l^T$ turns out to be a biased estimate of $\sum_{l=1}^L \mathcal{P}_l \mathcal{P}_l^T$.

For notational simplicity, denote $\bar{P}_l := \mathcal{P}_l - \text{diag}(\mathcal{P}_l)$ and denote $X_l := A_l - \bar{P}_l$. Then we can decompose the deviation of $\sum_{l=1}^L A_l A_l^T$ from $\sum_{l=1}^L \mathcal{P}_l \mathcal{P}_l^T$ as

$$\sum_{l=1}^L A_l A_l^T - \sum_{l=1}^L \mathcal{P}_l \mathcal{P}_l^T := N_1 + N_2 + N_3 + \text{diag}\left(\sum_{l=1}^L X_l X_l^T\right), \quad (5)$$

where

$$\begin{aligned} N_1 &= \sum_{l=1}^L \left(\text{diag}^2(\mathcal{P}_l) - \mathcal{P}_l \text{diag}(\mathcal{P}_l) - \text{diag}(\mathcal{P}_l) \mathcal{P}_l^T \right), \\ N_2 &= \sum_{l=1}^L (\bar{P}_l X_l^T + X_l \bar{P}_l^T), \\ N_3 &= \sum_{l=1}^L X_l X_l^T - \text{diag}\left(\sum_{l=1}^L X_l X_l^T\right). \end{aligned} \quad (6)$$

It turns out that N_1 , N_2 and N_3 are all relatively small. While for $\text{diag}(\sum_{l=1}^L X_l X_l^T)$, we have the following argument for its i th diagonal element,

$$\begin{aligned} \left(\text{diag}\left(\sum_{l=1}^L X_l X_l^T\right) \right)_{ii} &= \sum_{l=1}^L \sum_{j=1}^n X_{l,ij}^2 \\ &= \sum_{l=1}^L \sum_{j=1}^n [\bar{P}_{l,ij}^2 \mathbb{I}(A_{l,ij} = 0) + (1 - \bar{P}_{l,ij})^2 \mathbb{I}(A_{l,ij} = 1)] \\ &\leq L n \max_{l,ij} \bar{P}_{l,ij}^2 + \sum_{l=1}^L d_{l,i}^{\text{out}}, \end{aligned} \quad (7)$$

where $d_{l,i}^{\text{out}} := \sum_{j=1}^n A_{l,ij}$ is the out-degree of node i in layer l . Note that $\sum_{l=1}^L d_{l,i}^{\text{out}}$ has expectation $L n \max_{l,ij} \bar{P}_{l,ij}$, which results in that $\sum_{l=1}^L d_{l,i}^{\text{out}}$ is the dominant term in (7). As a result, we can directly remove the bias caused by $\sum_{l=1}^L d_{l,i}^{\text{out}}$. Specifically, define the row-wise

bias-adjusted SoG matrix by

$$S^R = \sum_{l=1}^L (A_l A_l^T - D_l^{out}), \quad (8)$$

where $D_l^{out} = \text{diag}(d_{l,1}^{out}, \dots, d_{l,n}^{out})$. Then, the row clusters partition can be obtained by performing k -means on the row of the K leading eigenvectors of S^R .

Similarly, for the column clusters, we can define the column-wise bias-adjusted SoG matrix by

$$S^C = \sum_{l=1}^L (A_l^T A_l - D_l^{in}), \quad (9)$$

where $D_l^{in} = \text{diag}(d_{l,1}^{in}, \dots, d_{l,n}^{in})$ with $d_{l,j}^{in} := \sum_{i=1}^n A_{l,ij}$. The column clusters partition can then be obtained by applying k -means on the row of the K' leading eigenvectors of S^C .

We summarize the spectral co-clustering based on the debiased SoG matrices in Algorithm 1, and in what follows, we will refer to the algorithm by DSoG.

Algorithm 1 Spectral co-clustering based on the debiased sum of Gram matrices (DSoG)

Input: Adjacency matrices A_1, \dots, A_L , row cluster number K_y , column cluster number K_z , target ranks $K (K \leq K_y)$ and $K' (K' \leq K_z)$;

Output: Estimated row membership matrix \hat{Y} , and column membership matrix \hat{Z} ;

- 1: Find the K leading eigenvectors \hat{U} of S^R in (8), and the K' leading eigenvectors \hat{V} of S^C in (9).
 - 2: Treat each row of \hat{U} as a point in $\mathbb{R}^{n \times K}$ and run the k -means with K_y clusters.
Treat each row of \hat{V} as a point in $\mathbb{R}^{n \times K'}$ and run the k -means with K_z clusters.
-

3.2 Consistency

We measure the quality of a clustering algorithm by the misclassification rate. Specifically, for the row clusters, it is defined as

$$\mathcal{L}(Y, \hat{Y}) = \min_{\Psi \in \Psi_{K_y}} \frac{1}{n} \|\hat{Y}\Psi - Y\|_0, \quad (10)$$

where $\hat{Y} \in \{0, 1\}^{n \times K_y}$ and Y correspond to the estimated and true membership matrices with respect to the row clusters, respectively, and Ψ_{K_y} is the set of all $K_y \times K_y$ permutation

matrices. Similarly, we can define the misclassification rate with respect to the column clusters by $\mathcal{L}(Z, \hat{Z})$.

To establish theoretical bounds on the misclassification rates, we need to pose assumption on B_l 's. We consider the rather general case where the aggregated squared link probability matrices $\sum_{l=1}^L B_l B_l^T$ and $\sum_{l=1}^L B_l^T B_l$ are allowed to be rank-deficient, where only a linear growth of their minimum *non-zero* eigenvalue is required. Specifically, we have the following Assumption 2.

Assumption 2. *The K th ($K \leq K_y$) non-zero eigenvalue of $\sum_{l=1}^L B_l B_l^T$ and the K' th ($K' \leq K_z$) non-zero eigenvalue of $\sum_{l=1}^L B_l^T B_l$ are at least $c_3 L$ for some constant $c_3 > 0$.*

Remark 3. *Compared with literature on multi-layer SBMs, see for example [Arroyo et al. \(2021\)](#); [Lei and Lin \(2022\)](#), Assumption 2 is much weaker. On the one hand, we do not require each B_l being of full rank, which is the benefit of combining layer-wise networks. On the other hand, the combined link probability matrix $\sum_{l=1}^L B_l B_l^T$ is also flexible to be degenerate.*

The following theorem provides an upper bound on the proportion of misclustered nodes in terms of row clusters under the multi-layer ScBM mentioned in Lemma 1.

Theorem 1. *Suppose that Assumptions 1 and 2, and (2) hold. If $L^{1/2} n \rho \geq c_4 \log(L + n)$ and $n \rho \leq c_5$ for positive constants c_4 and c_5 , then the output \hat{Y} of Algorithm 1 satisfies*

$$\mathcal{L}(Y, \hat{Y}) \leq \frac{c_6}{n \zeta_n^2} \left(\frac{1}{n^2} + \frac{\log(L + n)}{L n^2 \rho^2} \right) \quad (11)$$

with probability at least $1 - O((L + n)^{-1})$ for some constant $c_6 > 0$, where recall that ζ_n appears in (2).

Remark 4. *In Theorem 1, we considered a hard situation in single-layer ScBMs, where the layer-wise networks are rather sparse that $n \rho \leq c_5$ while the sparsity is alleviated with L networks in the sense that $L^{1/2} n \rho \geq c_4 \log(L + n)$. We can similarly derive the bound under several other settings.*

The proof of Theorem 1 is given in Appendix B. Theorem 1 shows that in certain sense, the number of layers L can boost the clustering performance. In addition, as expected, large

ζ_n would bring benefit to the clustering performance. In particular, if $\sum_{l=1}^L B_l B_l^T$ is of full rank, the RHS of 11 can be simplified to

$$c_7 \left(\frac{1}{n^2} + \frac{\log(L+n)}{Ln^2\rho^2} \right)$$

for some constant $c_7 > 0$.

Analogous to the row clusters, we provide the following results on the misclassification rate with respect to the column clusters.

Theorem 2. *Suppose that Assumptions 1 and 2, and (4) hold. If $L^{1/2}n\rho \geq c_8 \log(L+n)$ and $n\rho \leq c_9$ for positive constants c_8 and c_9 , then the output \hat{Z} of Algorithm 1 satisfies*

$$\mathcal{L}(Z, \hat{Z}) \leq \frac{c_{10}}{n\xi_n^2} \left(\frac{1}{n^2} + \frac{\log(L+n)}{Ln^2\rho^2} \right)$$

with probability at least $1 - O((L+n)^{-1})$ for some constant $c_{10} > 0$, where we recall that ξ_n appears in (4).

As the proof of Theorem 2 follows a similar approach to that of Theorem 1, it is omitted for brevity. Also, we can similarly discuss the results of Theorem 2.

4 Simulations

In this section, we evaluate the finite sample performance of the proposed algorithm DSoG. To this end, we perform three experiments. The first one corresponds to the case that $\sum_{l=1}^L B_l B_l^T$ is of full rank, while the second one corresponds to the rank-deficient case. The third one is designed to mimic typical directed network structures.

Methods for comparison. We compare our method DSoG with the following three methods.

- **Sum:** spectral co-clustering based on the *Sum* of adjacency matrices without squaring, that is, taking the left and right singular vectors of $\sum_{l=1}^L A_l$ as input of k -means clustering to obtain row and column clusters, respectively.

- **SoG**: spectral co-clustering based on the *Sum of Gram* matrices, that is, taking the eigenvectors of the non-debiased matrices $\sum_{l=1}^L A_l A_l^T$ and $\sum_{l=1}^L A_l^T A_l$ as the input of k -means clustering to obtain row and column clusters, respectively.
- **MASE**: the method called *Multiple Adjacency Spectral Embedding* (Arroyo et al., 2021), where to obtain row and column clusters, the eigenvectors of $\sum_{l=1}^L U_l U_l^T / L$ and $\sum_{l=1}^L V_l V_l^T / L$ are used as the input of the k -means clustering with U_l and V_l representing the singular vectors of the layer-wise matrices A_l .

Experiment 1. The networks are generated from the multi-layer ScBM via the mechanism given in (1). We consider $n = 500$ nodes per network across $K_y = 3$ row clusters and $K_z = 3$ column clusters, with row cluster sizes $n_1^y = 200$, $n_2^y = 100$, $n_3^y = 200$ and column cluster sizes $n_1^z = 150$, $n_2^z = 200$, $n_3^z = 150$. We fix $L = 50$ and set $B_l = \rho B^{(1)}$ for $l \in \{1, \dots, L/2\}$, and $B_l = \rho B^{(2)}$ for $l \in \{L/2 + 1, \dots, L\}$, with

$$B^{(1)} = U \begin{bmatrix} 1.5 & 0 & 0 \\ 0 & 0.2 & 0 \\ 0 & 0 & 0.4 \end{bmatrix} V^T \approx \begin{bmatrix} 0.46 & 0.625 & 0.225 \\ 0.46 & 0.225 & 0.625 \\ 0.85 & 0.46 & 0.46 \end{bmatrix}$$

and

$$B^{(2)} = U \begin{bmatrix} 1.5 & 0 & 0 \\ 0 & 0.2 & 0 \\ 0 & 0 & -0.4 \end{bmatrix} V^T \approx \begin{bmatrix} 0.46 & 0.225 & 0.625 \\ 0.46 & 0.625 & 0.225 \\ 0.85 & 0.46 & 0.46 \end{bmatrix},$$

where

$$U = \begin{bmatrix} 1/2 & 1/2 & -\sqrt{2}/2 \\ 1/2 & 1/2 & \sqrt{2}/2 \\ \sqrt{2}/2 & -\sqrt{2}/2 & 0 \end{bmatrix} \quad \text{and} \quad V = \begin{bmatrix} \sqrt{2}/2 & -\sqrt{2}/2 & 0 \\ 1/2 & 1/2 & -\sqrt{2}/2 \\ 1/2 & 1/2 & \sqrt{2}/2 \end{bmatrix}.$$

To measure the effect of network sparsity, we vary the overall edge density parameter ρ in the range of 0.03 to 0.16. It is obvious that direct summation of B_l would lead to the confusion of first and second clusters. Hence, it is expected that **Sum** would not perform well under this case.

Experiment 2. In this experiment, we consider the case where $\sum_{l=1}^L B_l B_l^T$ (or $\sum_{l=1}^L B_l B_l^T$) is rank-deficient. Specifically, we consider the following model. We fix $L = 50$ and set $B_l = \rho B^{(1)}$ for $l \in \{1, \dots, L/2\}$, and $B_l = \rho B^{(2)}$ for $l \in \{L/2 + 1, \dots, L\}$, with

$$B^{(1)} = U \begin{bmatrix} 1.2 & 0 & 0 \\ 0 & 0.4 & 0 \\ 0 & 0 & 0 \end{bmatrix} V^T = \begin{bmatrix} 0.59 & 0.14 & 0.33 \\ 0.14 & 0.39 & 0.47 \\ 0.33 & 0.47 & 0.63 \end{bmatrix}$$

and

$$B^{(2)} = U \begin{bmatrix} 1.2 & 0 & 0 \\ 0 & -0.4 & 0 \\ 0 & 0 & 0 \end{bmatrix} V^T = \begin{bmatrix} 0.01 & 0.46 & 0.52 \\ 0.46 & 0.21 & 0.37 \\ 0.52 & 0.37 & 0.57 \end{bmatrix},$$

where

$$U = V \approx \begin{bmatrix} 0.5 & 0.84 & -0.19 \\ 0.5 & -0.46 & -0.73 \\ 0.71 & -0.27 & 0.65 \end{bmatrix}$$

and ρ is the overall edge density parameter which varies from 0.03 to 0.16. It is easy to see that $\sum_{l=1}^L B_l B_l^T$ is rank-deficient and the rank is 2. As in Experiment 1, we consider $n = 500$ nodes per network across $K_y = 3$ row clusters and $K_z = 3$ column clusters, with row cluster sizes $n_1^y = 100$, $n_2^y = 150$, $n_3^y = 250$ and column cluster sizes $n_1^z = 150$, $n_2^z = 250$, $n_3^z = 100$. With this set-up, we generate the adjacency matrix with respect to each layer via (1).

Experiment 3. In this experiment, we generate directed networks with ‘transmission’ nodes or ‘message passing’ nodes. In networks with ‘transmission’ nodes, there exists a set of nodes that only receive edges from one set of nodes and send edges to another set of nodes, and hence are called ‘transmission nodes’. Hence, the sending clusters and receiving clusters are not the same. See Figure 1 (a) and (b) for illustration. In the network with ‘message passing’ the nodes, the edges spanning different communities start from upper communities down to lower communities, just like passing messages. See Figure 1(c) for illustration, where the row clusters and column clusters are identical. In our set-up, we fix $L = 30$ and set $B_l = \rho B^{(1)}$ for $l \in \{1, \dots, L/3\}$, $B_l = \rho B^{(2)}$ for $l \in \{L/3 + 1, \dots, 2L/3\}$, and $B_l = \rho B^{(3)}$

for $l \in \{2L/3 + 1, \dots, L\}$, with

$$B^{(1)} = \begin{bmatrix} 0.3 & 0 & 0 \\ 0 & 0.2 & 0 \\ 0 & 0 & 0.3 \end{bmatrix}, \quad B^{(2)} = \begin{bmatrix} 0 & 0 & 0 \\ 0.3 & 0 & 0 \\ 0.5 & 0.3 & 0 \end{bmatrix}, \quad B^{(3)} = \begin{bmatrix} 0 & 0.2 & 0.2 \\ 0 & 0 & 0.2 \\ 0 & 0 & 0 \end{bmatrix}.$$

Under $B^{(1)}$, we let the row and column clusters to be different with transmission nodes; see Figure 1 (a) and (b) for illustration. Under $B^{(2)}$ and $B^{(3)}$, we incorporate the message passing nodes and the row clusters and column clusters are identical to those corresponds to $B^{(1)}$; see Figure 1 (c) for illustration. Specifically, we consider $n = 300$ nodes per network across $K_y = 3$ row clusters and $K_z = 3$ column clusters, with row cluster sizes $n_1^y = 120$, $n_2^y = 100$, $n_3^y = 80$ and column cluster sizes $n_1^z = 80$, $n_2^z = 100$, $n_3^z = 120$. With this set-up, we generate the adjacency matrix for each layer via (1), with the overall edge density parameter ρ varying from 0.03 to 0.16.

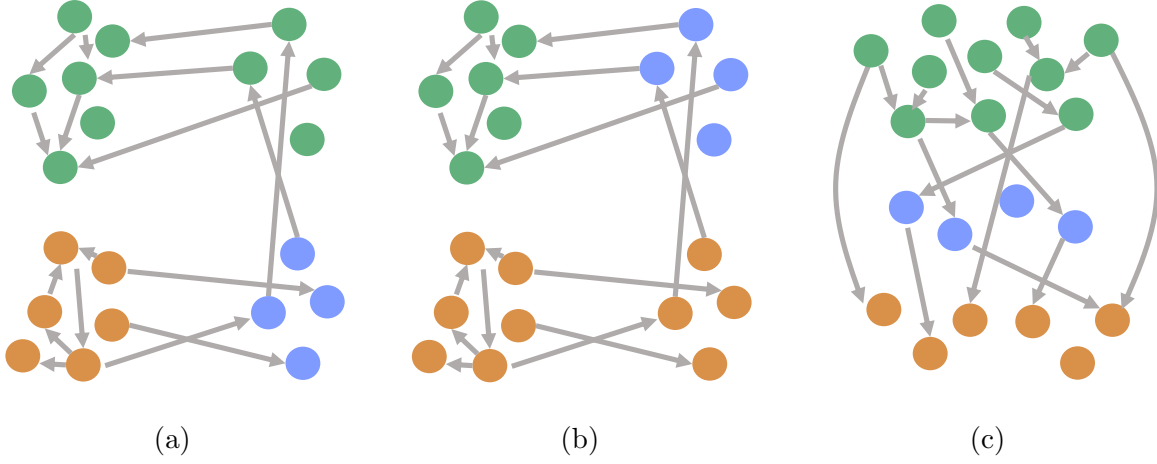
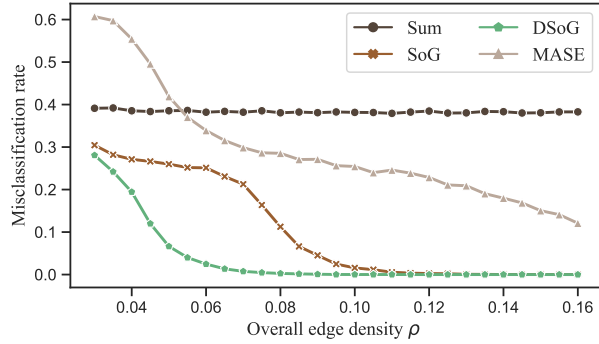
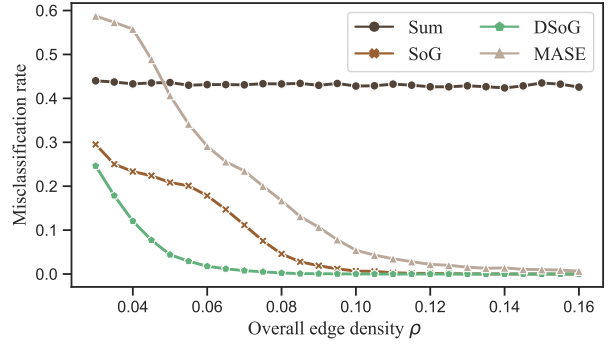


Figure 1: Illustration for networks under different link probability matrices. Colors indicate communities. (a) row clusters under $B^{(1)}$; (b) column clusters under $B^{(1)}$; (c) Row clusters under $B^{(2)}$ ($B^{(3)}$); column clusters are analogous.

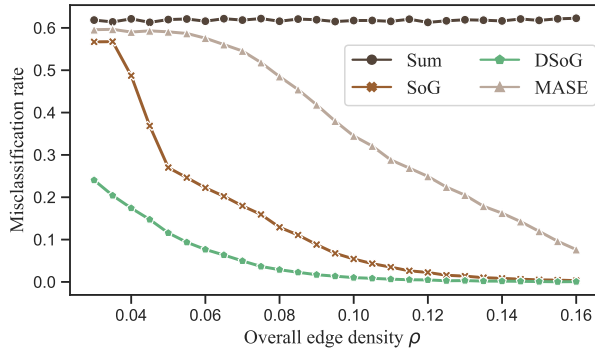
Results. We use the misclassification rate defined in (10) to measure the proportion of misclassified (up to permutations) nodes. The averaged results over 50 replications for Experiments 1-3 are displayed in Figure 2, where we vary ρ from 0.03 to 0.16 in 27 equally-spaced values. The results demonstrate that our proposed method DSoG has a noticeable



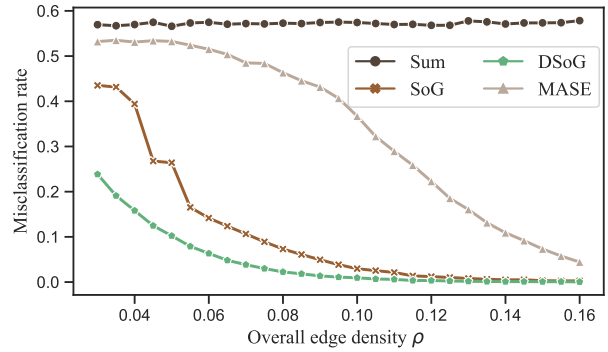
(a) Experiment 1, row clustering



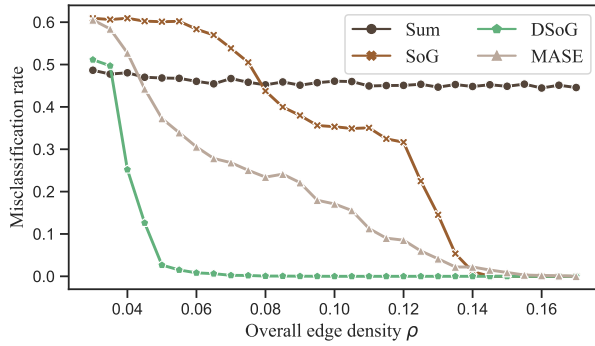
(b) Experiment 1, column clustering



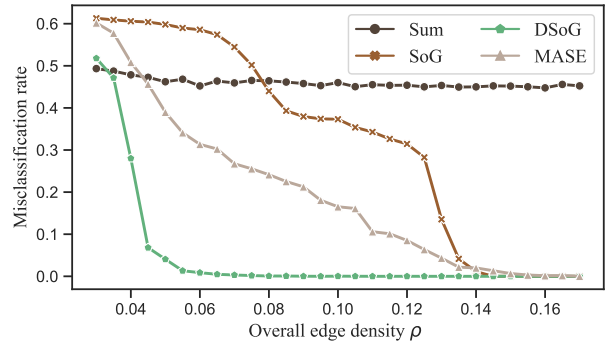
(c) Experiment 2, row clustering



(d) Experiment 2, column clustering



(e) Experiment 3, row clustering



(f) Experiment 3, column clustering

Figure 2: Misclassification rates of four methods with varying ρ in three experimental setups. The horizontal directions correspond to Experiments 1-3 sequentially, and the vertical directions correspond to the performance with respect to the row clusters and column clusters, respectively.

impact on the accuracy of clustering. Specifically, the **Sum** method performs poorly due to the fact that some eigen-components cancel out in the summation. The **DSoG** method has a significant advantage over the **SoG** method, especially when ρ is small, i.e., the very sparse regime, which is consistent with our theoretical results. We can also observe that our method **DSoG** outperforms the **MASE** method in all settings.

5 Real data analysis

In this section, we analyze the WFAT dataset, which is a public dataset collected by the Food and Agriculture Organization of the United Nations. The original data includes trading records for more than 400 food and agricultural products imported/exported annually by all the countries in the world. The dataset is available at <https://www.fao.org>. As described in other works analyzing these data (De Domenico et al., 2015; Jing et al., 2021; Noroozi and Pensky, 2022), it can be considered as a multi-layer network, where layers represent food and agricultural products, and nodes are countries and edges at each layer represent import/export relationships of a specific food and agricultural product among countries. Jing et al. (2021) and Noroozi and Pensky (2022) partitioned the layers into groups, where the layers within a certain group can be assumed to have networks with common community structures. Thus, we focus on the group obtained by Noroozi and Pensky (2022) to show that our method can produce insightful national communities; see Table 1 for the products we considered.

Data preprocessing. We convert the original trading data into directed networks, which is distinct from all previously described efforts to analyze this data, where the trading data is reduced to an undirected network. We focus on the trading data in year 2020. To create a directed trading network for each of the 24 products, we draw a directed edge from the exporter to the importer if the export/import value of the product exceeds \$10000. This particular threshold would yield sparse networks that have many disjoint connected components individually but have one connected component after aggregation. We then removed all the countries (nodes) whose total in-degree or out-degree across all 24 layers is

<p>“Pastry”, “Rice, paddy”, “Rice, milled”, “Breakfast cereals”, Mixes and doughs”, “Food preparations of flour, meal or malt extract”, “Sugar and syrups n.e.c.”, “Sugar confectionery”, “Communion wafers and similar products.”, “Prepared nuts”, “Vegetables preserved (frozen)”, “Juice of fruits n.e.c.”, “Fruit prepared n.e.c.”, “Orange juice”, “Other non-alcoholic caloric beverages”, “Food wastes”, “Other spirituous beverages”, “Coffee, decaffeinated or roasted”, “Coffee, green”, “Chocolate products nes”, “Pepper, raw”, “Dog or cat food, put up for retail sale”, “Food preparations n.e.c.”, “Crude organic material n.e.c.”</p>
--

Table 1: List of a group of food and agricultural products obtained by [Noroozi and Pensky \(2022\)](#), which consists of 24 different products involving cereals, stimulant crops, and derived products.

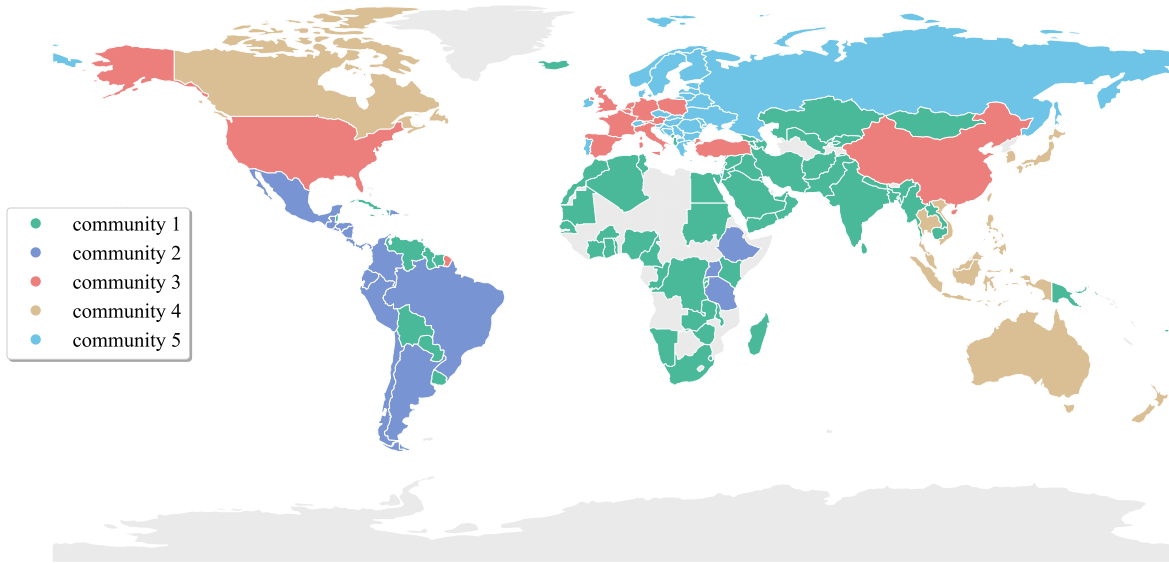
less than 14. We choose this value to make sure that each node has links to at least one of the other nodes in at least half of the layers. Indeed, the average total in-degree and out-degree of nodes which do not have any neighbors in 12 or more of the layers (i.e., more than half of the layers have a zero out-degree or in-degree) is 13. As a result, we obtain a multi-layer network with 24 layers and 142 nodes per layer. Subsequently, we reconstruct the row and column clusters using the proposed algorithm. For this purpose, we choose $K_y = 5$ and $K_z = 5$, which is consistent with the number of continents (Asia, Europe, America, Africa and Oceania).

Results. The estimated row and column clusters are displayed in Figure 3. The clusters of countries are approximately related to their geographic locations, which is coherent with the economic laws of world trade. Specifically, for the row clusters (see Figure 3(a)), Community 1 mainly includes countries in Africa, West, Central and South Asia; Community 2 is composed of countries in Central and South America; Community 3 includes China, the United States, Western and Southern Europe countries; Community 4 involves Southeast Asia and Oceania countries; Community 5 consists of the remaining European countries. For the column clusters (see Figure 3(b)), Community 1 mainly includes Africa and West Asia countries; Community 2 consists of countries in Central and South America; Commu-

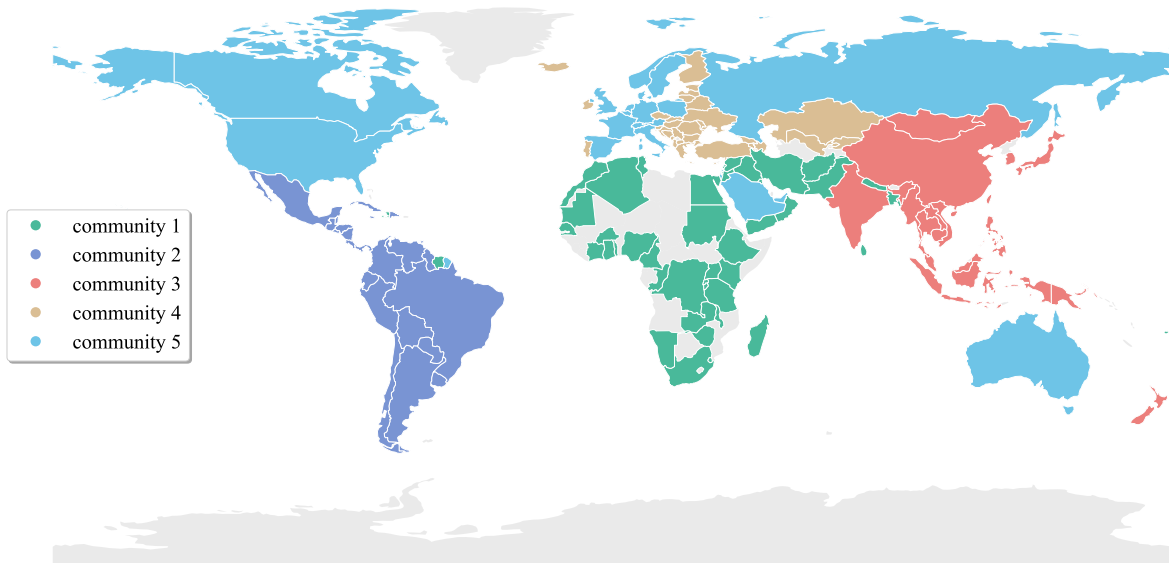
nity 3 includes East and South Asia countries; Community 4 involves Eastern European and some West Asian countries; Community 5 mainly includes Western Europe, North America, Australia and Russia.

We can see that the structure of the row (export) clusters is not identical to that of the column (import) clusters, which is insightful and more realistic than what would be expected from undirected multi-layer networks. For instance, China is grouped with major European economies and America in the row clusters partition, while it is grouped mainly with East and South Asia countries in the column clusters partition, indicating that for the products in Table 1, China is aligned with major world economies in its export trade, while it is aligned mainly with neighboring countries in its import trade. This observation is entirely plausible. Export patterns primarily reflect a nation’s productive capacity and dominant industries. Major global economies with robust food processing industries and agricultural technology tend to export value-added manufactured goods. Conversely, import patterns primarily mirror a country’s consumer demand. Due to similar geographical conditions, population sizes and food consumption habits, countries in close proximity to each other often exhibit similar import patterns. In contrast, we consider the process of transforming directed graphs into undirected graphs, as mentioned in the introduction, which leads to the clustering results shown in Figure 4. Ignoring the directionality of the edges, the clustering outcome aligns closely with that of the export patterns. This is attributed to the fact that export activities often play a more proactive and decisive role in a nation’s trade patterns. Exports illuminate factors such as a country’s industrial organization, competitiveness, and position in the global value chain. If the export pattern of one country mirrors that of another, they may also show similarities in their overall trade patterns. This could lead to a failure to recognize the unique characteristics of import patterns and thus to a less comprehensive understanding of trade relations.

Visualizations of the aggregated adjacency matrix and several single-layer adjacency matrices are also presented, which can illustrate the advantages of multi-layer networks and further highlight the difference between sending and receiving patterns. Figure 5 illustrates the network of the products listed in Table 1, aggregated in a summation manner. In Figure 6, the adjacency matrices for the six products featured in Table 1 are displayed. To highlight



(a) row (export) clustering



(b) column (import) clustering

Figure 3: Community structure separation of food trade networks (directed) containing 142 major countries. Colors indicate communities, where light gray corresponds to countries that do not participate in clustering.

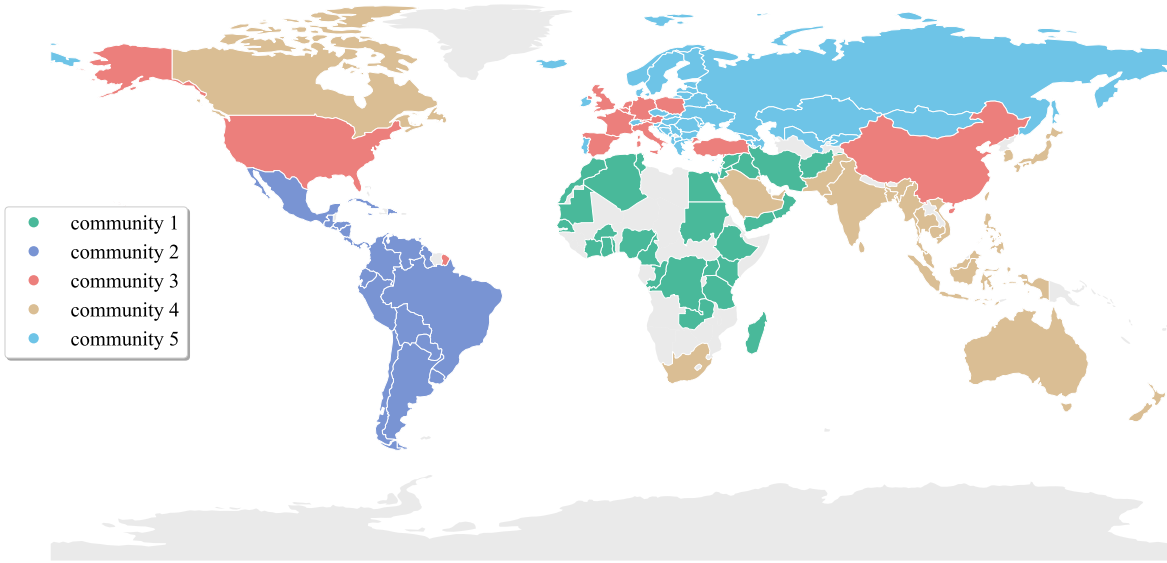


Figure 4: Community structure separation of food trade networks (undirected) containing 142 major countries. Colors indicate communities, where light gray corresponds to countries that do not participate in clustering.

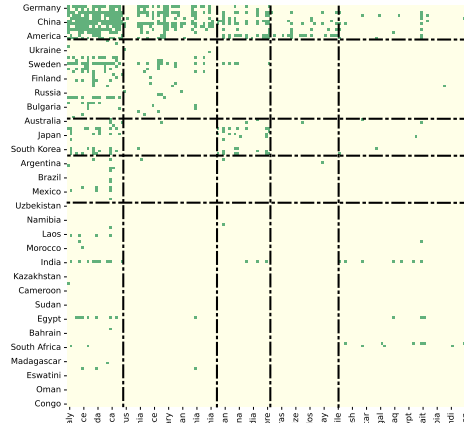
the clustering outcomes, the order of the nodes (countries) is adjusted accordingly and persists in each plot. Due to space limitations, only a portion of the countries are labeled on the axes. It is clear that our clustering results have a significant community structure, and the row (export) clusters are quite different from the column (import) clusters, as reflected by the fact that the row and column clusters in the same country have distinctly different compositions and different community sizes. Such asymmetric information cannot be captured by undirected networks. More significantly, a comparison between the individual adjacency matrices in Figure 6 and Figure 5 reveals that a single-layer network only encapsulates a fraction of the community structure information, and a more comprehensive picture of trade relations among countries can be obtained by aggregating the individual trade networks for multiple products. This aligns with our original intention of dealing with multi-layer directed networks.



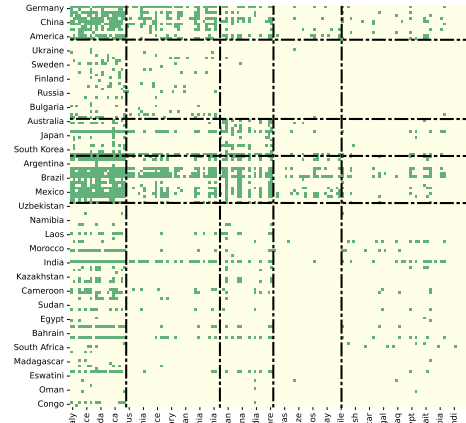
Figure 5: Visualization of the aggregated adjacency matrix. Yellow pixels correspond to the absence of an edge between the corresponding countries while green pixels correspond to an edge. The black dashed lines in the figures signifies the division between clusters.

6 Conclusion

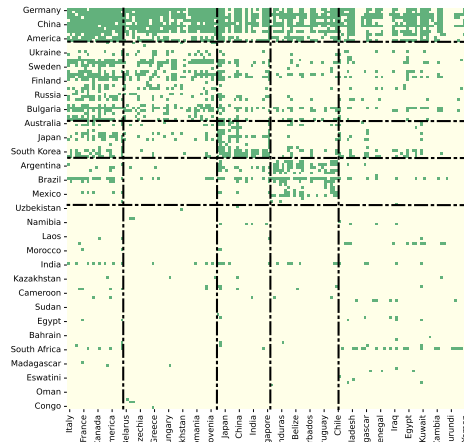
In this paper, we studied the problem of detecting co-clusters in multi-layer directed networks. We typically assumed that the multi-layer directed network is generated from the multi-layer ScBM, which allows different row and column clusters via different patterns of sending and receiving edges. The proposed method **DSoG** is formulated as the spectral co-clustering based on the SoG matrices of the row and column spaces, where a bias correction step is implemented. We systematically studied the algebraic properties of the population version of **DSoG**. In particular, we did not require that the corresponding link probability matrix be of full rank. We also studied the misclassification error rates of **DSoG**, which show that under certain condition, multiple layers can bring benefit to the clustering performance. We finally conducted numerical experiments on a number of simulated and real examples to support the theoretical results.



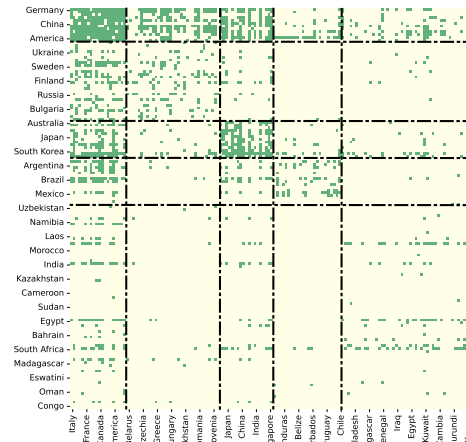
(a) Vegetables preserved (frozen)



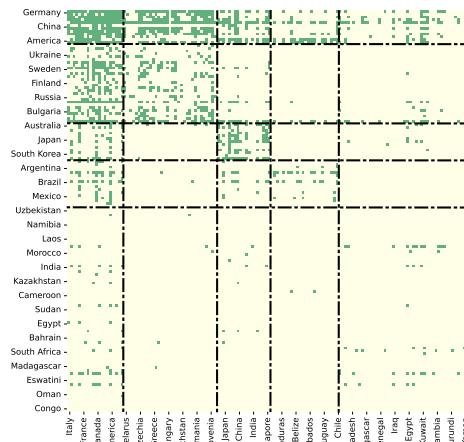
(b) Coffee, green



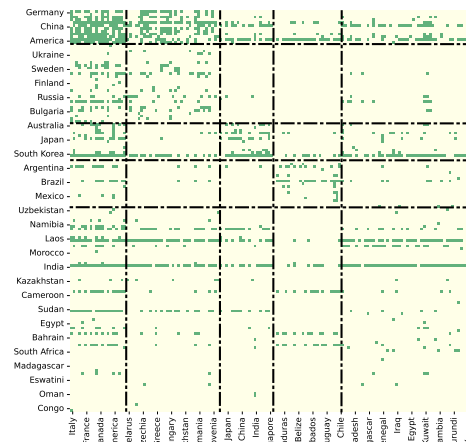
(c) Food wastes



(d) Juice of fruits n.e.c.



(e) Coffee, decaffeinated or roasted



(f) Rice, paddy

Figure 6: Visualization of the adjacency matrices for six products. The colors, node order, and community partition are identical to Figure 5.

There are many ways to extend the content of this paper. First, we focused on the scenario where the layer-wise community structures are homogeneous. It is of great interest to extend the scenario to associated but inhomogeneous community structures, which has been studied recently for multi-layer undirected networks (Han et al., 2015; Pensky and Zhang, 2019; Chen et al., 2022). Second, we analyzed the WFAT dataset with respect to a particular year. However, this dataset contains the annual trading data from 1986 to the present and is continuously updated, which actually constitutes a *higher-order* multi-layer network that contains more adequate information than a single multi-layer network. It is thus of great importance to develop a corresponding toolbox for this higher-order multi-layer network. Third, it is important to study the estimation of the number of communities (Fishkind et al., 2013; Ma et al., 2022).

Appendix

Appendix A provides the technical theorem and lemma that are needed to prove the misclassification rates. Appendix B includes the proof of main theorem and lemmas in the main text. Appendix C contains auxiliary lemmas.

A Technical theorem and lemma

Theorem 3. *Let $A_l \in \{0, 1\}^{n \times n}$ be the adjacency matrices generated by a multi-layer ScBM and $X_l = A_l - \bar{P}_l$ be the asymmetric noise matrices for all $1 \leq l \leq L$, where $\bar{P}_l = \mathbb{E}(A_l)$. If $L^{1/2}n\rho \geq c_1 \log(L+n)$ and $n\rho \leq c_2$ for positive constants c_1 and c_2 , then E_1 , the off-diagonal part of $\sum_{l=1}^L X_l X_l^T$, satisfies*

$$\|E_1\|_2 \leq cL^{1/2}n\rho \log^{1/2}(L+n)$$

with probability at least $1 - O((L+n)^{-1})$ for some constant $c > 0$.

To handle the complicated dependence in E_1 caused by the quadratic form, the key idea in the proof is viewing E_1 as a matrix-valued U-statistic with a centered kernel function of order two, indexed by the pairs (i, j) , and using the decoupling technique described in Lemma

8, which reduces problems on dependent variables to problems on related (conditionally) independent variables. This type of proof technique is also used in [Lei and Lin \(2022\)](#), dealing with the symmetric case. Specifically, rearrange E_1 as

$$E_1 = \sum_{l=1}^L \sum_{(i,j) \neq (i',j')} X_{l,ij} X_{l,i'j'} e_i e_{i'}^T I_{\{j=j'\}}, \quad (12)$$

where e_i is the standard basis vector in \mathbb{R}^n and pairs $(i,j), (i',j') \in \{1, 2, \dots, n\}^2$, which can be viewed as a matrix-valued U-statistic defined on the vectors $X_{1,ij}, \dots, X_{L,ij}$ indexed by the pairs (i,j) . The decoupling technique reduces the problem of bounding $\|E_1\|_2$ to that of bounding $\|\sum_{l=1}^L X_l \tilde{X}_l^T\|_2$ and $\|\text{diag}(\sum_{l=1}^L X_l \tilde{X}_l^T)\|_2$, where \tilde{X}_l is an independent copy of X_l for all $1 \leq l \leq L$.

Proof. To use the decoupling argument, define

$$\begin{aligned} \tilde{E}_1 &= \sum_{l=1}^L \sum_{(i,j) \neq (i',j')} X_{l,ij} \tilde{X}_{l,i'j'} e_i e_{i'}^T I_{\{j=j'\}}, \\ \tilde{E}_2 &= \sum_{l=1}^L \sum_{(i,j)} X_{l,ij} \tilde{X}_{l,ij} e_i e_i^T, \end{aligned}$$

and

$$\tilde{E} = \sum_{l=1}^L X_l \tilde{X}_l^T = \tilde{E}_1 + \tilde{E}_2.$$

where \tilde{E}_1 is the zero mean off-diagonal part and \tilde{E}_2 is the diagonal part. Note that $\|\tilde{E}_1\|_2 \leq \|\tilde{E}\|_2 + \|\tilde{E}_2\|_2$, we control the spectral norm of \tilde{E} and \tilde{E}_2 separately.

First step: Controlling \tilde{E} . Recall that $\tilde{X}_l = \tilde{A}_l - \bar{P}_l$, where \tilde{A}_l is an independent copy of A_l , we reformulate \tilde{E} as

$$\tilde{E} = \sum_{l=1}^L X_l \tilde{X}_l^T = \sum_{l=1}^L X_l \tilde{A}_l^T - \sum_{l=1}^L X_l \bar{P}_l^T.$$

Applying Lemma 6 with $(v, b) = (2\rho, 1)$, if $L^{1/2} n \rho^{1/2} \geq c_1 \log^{1/2}(L+n)$ for some constant $c_1 > 0$, we have with probability at least $1 - O((L+n)^{-1})$ and universal constant $c > 0$,

$$\left\| \sum_{l=1}^L X_l \bar{P}_l^T \right\|_2 \leq c L^{1/2} n^{3/2} \rho^{3/2} \log^{1/2}(n+L). \quad (13)$$

Note that the constant c may be different from line to line in this proof.

In order to apply Lemma 6 to control $\sum_{l=1}^L X_l \tilde{A}_l^T$ conditioning on $\tilde{A}_1, \dots, \tilde{A}_L$, we need to upper bound $\max_l \|\tilde{A}_l^T\|_{2,\infty}$, $\sum_{l=1}^L \|\tilde{A}_l^T\|_F^2$ and $\|\sum_{l=1}^L \tilde{A}_l \tilde{A}_l^T\|_2$, respectively. Note that \tilde{A}_l is an independent copy of A_l , now we bound the corresponding version of A_l .

We first consider $\max_l \|A_l^T\|_{2,\infty}$. Note that $\mathbb{E}d_{l,i}^{in} \leq n\rho$. Applying a union bound over $i \in [n]$ and $l \in [L]$, along with the standard Bernstein's inequality

$$\mathbb{P}(d_{l,i}^{in} - \mathbb{E}d_{l,i}^{in} \geq t) \leq \exp\left(-\frac{t^2/2}{n\rho + t}\right)$$

for all $t > 0$, and using the assumption that $n\rho \leq c_2$, then with probability at least $1 - O((L+n)^{-1})$, we have

$$\max_l \|A_l^T\|_{2,\infty} = \max_{l,i} \sqrt{d_{l,i}^{in}} \leq c \log^{1/2}(L+n). \quad (14)$$

For $\sum_{l=1}^L \|A_l^T\|_F^2$, using Bernstein's inequality for $\sum_{l=1}^L d_{l,i}^{in}$ and the assumption that $L^{1/2}n\rho \geq c_1 \log(L+n)$, we have with probability at least $1 - O((L+n)^{-1})$,

$$\sum_{l=1}^L \|A_l^T\|_F^2 \leq n \max_i \sum_{l=1}^L d_{l,i}^{in} \leq cLn^2\rho. \quad (15)$$

Now we turn to $\|\sum_{l=1}^L A_l A_l^T\|_2$. To begin with, decompose $\sum_{l=1}^L A_l A_l^T$ as $F_1 + F_2$, where F_1 is the off-diagonal part, which can be viewed as a matrix-valued U-statistic as in (12), and F_2 is the diagonal part. For the off-diagonal part F_1 , \tilde{F}_1 is defined as the off-diagonal part of $\sum_{l=1}^L A_l \tilde{A}_l^T$ for the purpose of using the decoupling technique. Using symmetrization and Perron-Frobenius theorem, we have

$$\|\tilde{F}_1\|_2 = \left\| \begin{pmatrix} 0 & \tilde{F}_1 \\ \tilde{F}_1^T & 0 \end{pmatrix} \right\|_2 \leq \max \left\{ \|\tilde{F}_1\|_{1,\infty}, \|\tilde{F}_1^T\|_{1,\infty} \right\} \leq \max \left\{ \left\| \sum_{l=1}^L A_l \tilde{A}_l^T \right\|_{1,\infty}, \left\| \sum_{l=1}^L \tilde{A}_l A_l^T \right\|_{1,\infty} \right\}.$$

By simple calculations, the l_1 norm of the i th row of $\sum_{l=1}^L A_l \tilde{A}_l^T$ is $\sum_{l=1}^L \sum_{j=1}^n A_{l,ij} \tilde{d}_{l,j}^{in}$. Combining (14) and (15) with Bernstein's inequality, we have

$$\begin{aligned} & \mathbb{P} \left(\sum_{l=1}^L \sum_{j=1}^n A_{l,ij} \tilde{d}_{l,j}^{in} - \sum_{l=1}^L \sum_{j=1}^n \mathbb{E}(A_{l,ij}) \tilde{d}_{l,j}^{in} \geq t \mid \tilde{A}_1, \dots, \tilde{A}_L \right) \\ & \leq \exp \left(-\frac{t^2/2}{cLn^2\rho^2 \log(L+n) + c \log(L+n)t} \right) \end{aligned}$$

for all $t > 0$. By applying the total probability theorem, the union bound, and the assumption that $L^{1/2}n\rho \geq c_1 \log(L+n)$, we have with high probability, $\max_i \sum_{l=1}^L \sum_{j=1}^n A_{l,ij} \tilde{d}_{l,j}^{in} \leq$

$cL^{1/2}n\rho\log(L+n) \leq cLn^2\rho^2$. A similar argument is conducted for $\sum_{l=1}^L \tilde{A}_l A_l^T$. By Lemma 8 we have

$$\|F_1\|_2 \leq cLn^2\rho^2 \quad (16)$$

with high probability. For the diagonal part F_2 , applying (15), we have

$$\|F_2\|_2 = \max_i \sum_{l=1}^L d_{l,i}^{out} \leq cLn\rho \quad (17)$$

with high probability. Combining (16), (17) with the assumption that $n\rho \leq c_2$, we have with probability at least $1 - O((L+n)^{-1})$,

$$\left\| \sum_{l=1}^L A_l A_l^T \right\|_2 \leq cLn\rho.$$

So combining the bounds for $\max_l \|\tilde{A}_l^T\|_{2,\infty}$, $\sum_{l=1}^L \|\tilde{A}_l^T\|_F^2$ and $\|\sum_{l=1}^L \tilde{A}_l \tilde{A}_l^T\|_2$, and applying Lemma 6, we have with probability at least $1 - O((L+n)^{-1})$,

$$\left\| \sum_{l=1}^L X_l \tilde{A}_l^T \right\|_2 \leq cL^{1/2}n\rho\log^{1/2}(L+n).$$

Combining this with (13), we have with probability at least $1 - O((L+n)^{-1})$,

$$\|\tilde{E}\|_2 \leq cL^{1/2}n\rho\log^{1/2}(L+n).$$

Second step: Controlling \tilde{E}_2 . Recall that \tilde{E}_2 is a diagonal matrix whose i th diagonal element is $\sum_{l=1}^L \sum_{j=1}^n X_{l,ij} \tilde{X}_{l,ij}$. Using standard Bernstein's inequality and union bound, we have with probability at least $1 - O((L+n)^{-1})$,

$$\|\tilde{E}_2\|_2 \leq cL^{1/2}n\rho\log^{1/2}(L+n).$$

The claim follows by combining the bounds for $\|\tilde{E}\|_2$ and $\|\tilde{E}_2\|_2$ together with the decoupling inequality in Lemma 8. \square

Lemma 5. *Let H be an $n \times s$ matrix with full column rank and the s th eigenvalue of HH^T is at least h for some constant $h > 0$. Let G be an $s \times s$ symmetric matrix with $\text{rank}(G) = j \leq s$ and the j th eigenvalue of G is at least g for some constant $g > 0$. Then $\lambda_j(HGH^T) \geq hg$.*

Proof. Note that $\text{rank}(H) = s$, we have $\dim\{x \in \mathbb{R}^n \mid x \perp \text{null}(H^T)\} = s$, where $\text{null}(H^T)$ is the nullspace of H^T and is given by $\text{null}(H^T) := \{\theta \in \mathbb{R}^n \mid H^T \theta = 0\}$. Combining this with $\text{rank}(G) = j$, we have $\dim\{x \in \mathbb{R}^n \mid x \perp \text{null}(H^T), H^T x \perp \text{null}(G)\} = s$. Thus

$$\min_{x \in \mathbb{R}^n, x \perp \text{null}(H^T), H^T x \perp \text{null}(G)} \frac{x^T H G H^T x}{x^T x} \geq g \cdot \min_{x \in \mathbb{R}^n, x \perp \text{null}(H^T)} \frac{x^T H H^T x}{x^T x} \geq h g.$$

Applying the Courant-Fischer minimax theorem (Theorem 8.1.2 of [Golub and Van Loan \(2013\)](#)), intersecting on this event, we have

$$\lambda_j(H G H^T) = \max_{\dim(\mathcal{H})=j} \min_{0 \neq x \in \mathcal{H}} \frac{x^T H G H^T x}{x^T x} \geq h g,$$

where \mathcal{H} is the subspace of \mathbb{R}^n . The proof is completed. \square

B Main proofs

Proof of Theorem 1

We decompose the matrix S^R into the sum of a signal term and noise terms.

Recall that $\mathcal{P}_l = \rho Y B_l Z^T$ and $\bar{\mathcal{P}}_l = \mathcal{P}_l - \text{diag}(\mathcal{P}_l)$. Define

$$N_4 = \text{diag}\left(\sum_{l=1}^L X_l X_l^T\right) - \sum_{l=1}^L D_l^{\text{out}}$$

and recall the definition of S^R in (8) and the decomposition (5), we have

$$S^R = \sum_{l=1}^L \mathcal{P}_l \mathcal{P}_l^T + N_1 + N_2 + N_3 + N_4.$$

We first control the signal term. Recall that $\Delta_z = \text{diag}(\sqrt{n_1^z}, \dots, \sqrt{n_{K_z}^z})$ is a $K_z \times K_z$ diagonal matrix, then $Z = \tilde{Z} \Delta_z$ with \tilde{Z} being a column orthogonal matrix. By the balanced community sizes assumption and the number of column clusters K_z is fixed, the minimum eigenvalue of Δ_z is lower bounded by $c_0 n^{1/2}$ for some constant $c_0 > 1$. Then we have

$$\sum_{l=1}^L \mathcal{P}_l \mathcal{P}_l^T = \rho^2 \sum_{l=1}^L Y B_l \Delta_z \tilde{Z}^T \tilde{Z} \Delta_z B_l^T Y^T \succeq c_0 n \rho^2 Y \left[\sum_{l=1}^L B_l B_l^T \right] Y^T,$$

where \succeq denotes the Loewner partial order, in particular, let A and B be two Hermitian matrices of order p , we say that $A \succeq B$ if $A - B$ is positive semi-definite. Note that Y is of

full column rank and the K_y th (and smallest) non-zero eigenvalue of YY^T is lower bounded by $c_0 n$ for some constant c_0 , where we used the balanced community sizes assumption and the number of row clusters K_y is fixed. Using Lemma 5 and Assumption 2, we can lower bound the K th eigenvalue of $\sum_{l=1}^L \mathcal{P}_l \mathcal{P}_l^T$ to be

$$\lambda_K(\sum_{l=1}^L \mathcal{P}_l \mathcal{P}_l^T) \geq c L n^2 \rho^2$$

for some constant $c > 0$. Note that we use c_0, c_1, c_2 and c to represent the generic constants and they may be different from line to line.

Then we bound each noise term respectively. The first noise term N_1 is non-random and satisfies

$$\|N_1\|_2 \leq n \|N_1\|_{\max} \leq L n \rho^2.$$

For N_2 , recalling that $X_l = A_l - \bar{P}_l$, where $X_{l,ij} (1 \leq i, j \leq n)$ is generated independently from centered Bernoulli, and is therefore $(2\rho, 1)$ -Bernstein. Using Lemma 6 and the fact that $\|\bar{P}_l^T \bar{P}_l\|_2 \leq n^2 \rho^2$, $\|\bar{P}_l\|_2 \leq n^2 \rho^2$ and $\|\bar{P}_l\|_{2,\infty} \leq n^{1/2} \rho$, if $L^{1/2} n \rho^{1/2} \geq c_1 \log^{1/2}(L+n)$ for some constant $c_1 > 0$, we have with probability at least $1 - O((L+n)^{-1})$ and universal constant $c > 0$,

$$\|N_2\|_2 \leq c L^{1/2} n^{3/2} \rho^{3/2} \log^{1/2}(n+L).$$

For the noise term N_3 , applying Theorem 3, we have

$$\|N_3\|_2 \leq c L^{1/2} n \rho \log^{1/2}(L+n)$$

with probability at least $1 - O((L+n)^{-1})$.

We next control N_4 . The construction in (7) implies that

$$\|N_4\|_2 \leq L n \rho^2.$$

Let U and \hat{U} be the $n \times K$ matrices consisting of the leading eigenvectors of $\sum_{l=1}^L \mathcal{P}_l \mathcal{P}_l^T$ and S^R , respectively. We are now ready to bound the derivation of \hat{U} from U . Combining the lower bound of signal term and upper bound of all noise terms, we have with high probability,

$$\frac{\|N_1 + N_2 + N_3 + N_4\|_2}{\lambda_K(\sum_{l=1}^L \mathcal{P}_l \mathcal{P}_l^T)} \leq c \frac{L n \rho^2 + L^{1/2} n \rho \log^{1/2}(L+n)}{L n^2 \rho^2}$$

$$\leq \frac{c}{n} + \frac{c \log^{1/2}(L+n)}{L^{1/2}n\rho},$$

where the first inequality arises from the merging of the N_2 and N_3 terms when $n\rho \leq c_2$ for some constant $c_2 > 0$. By Proposition 2.2 of [Vu and Lei \(2013\)](#) and Davis-Kahan $\sin\Theta$ theorem (Theorem VII.3.1 of [Bhatia \(1997\)](#)), there exists a $K \times K$ orthogonal matrix O such that

$$\begin{aligned} \|\widehat{U} - UO\|_F &\leq \sqrt{K} \|\widehat{U} - UO\|_2 \\ &\leq \frac{\sqrt{K} \|N_1 + N_2 + N_3 + N_4\|_2}{\lambda_K(\sum_{l=1}^L \mathcal{P}_l \mathcal{P}_l^T) - \|N_1 + N_2 + N_3 + N_4\|_2} \\ &\lesssim \frac{1}{n} + \frac{\log^{1/2}(L+n)}{L^{1/2}n\rho}, \end{aligned}$$

where $a_n \lesssim b_n$ means that there exists some positive constant c such that $a_n \leq cb_n$ for all n . Finally, by using Lemma 7, we are able to obtain the desired bound for the misclassification rate.

Proof of Lemma 1

Define $\Delta_y = \text{diag}(\sqrt{n_1^y}, \dots, \sqrt{n_{K_y}^y})$ as a $K_y \times K_y$ diagonal matrix with k th diagonal entry being the l_2 norm of the k th column of Y . Then $Y\Delta_y^{-1}$ is a column orthogonal matrix. Similarly define $\Delta_z = \text{diag}(\sqrt{n_1^z}, \dots, \sqrt{n_{K_z}^z})$. Write \mathcal{P}^R as

$$\begin{aligned} \mathcal{P}^R &= \rho^2 Y \sum_{l=1}^L B_l Z^T Z B_l^T Y^T \\ &= \rho^2 Y \Delta_y^{-1} \Delta_y \sum_{l=1}^L B_l \Delta_z^2 B_l^T \Delta_y \Delta_y^{-1} Y^T = \rho^2 Y \Delta_y^{-1} Q^R D^R Q^{R^T} \Delta_y^{-1} Y^T, \end{aligned}$$

where we used the eigen-decomposition of $\Delta_y \sum_{l=1}^L B_l \Delta_z^2 B_l^T \Delta_y$ is $Q^R D^R Q^{R^T}$. Here Q^R is a $K_y \times K$ column orthogonal matrix and D^R is a $K \times K$ diagonal matrix, which is due to the fact that $Z^T Z$ is a positive definite diagonal matrix, and hence the rank of $\sum_{l=1}^L B_l B_l^T$ is equal to the rank of $\Delta_y \sum_{l=1}^L B_l \Delta_z^2 B_l^T \Delta_y$.

It is easy to see that $Y\Delta_y^{-1}Q^R$ has orthogonal columns, so we have

$$U = Y\Delta_y^{-1}Q^R. \tag{18}$$

When $\sum_{l=1}^L B_l B_l^T$ is of full rank, that is, $K = K_y$, $\Delta_y^{-1} Q^R$ is invertible, thus $Y_{i*} = Y_{j*}$ if and only if $U_{i*} = U_{j*}$. The first claim follows by the fact that the rows of $\Delta_y^{-1} Q^R$ are perpendicular to each other and the k th row has length $\sqrt{n_k^y}$.

When $\sum_{l=1}^L B_l B_l^T$ is rank-deficient, that is, $K < K_y$, $Y_{i*} = Y_{j*}$ can also imply $U_{i*} = U_{j*}$ by (18). On the other hand, by (18), $\|U_{i*} - U_{j*}\|_2 := \left\| \frac{Q_{g_i^y}^R}{\sqrt{n_{g_i^y}}} - \frac{Q_{g_j^y}^R}{\sqrt{n_{g_j^y}}} \right\|_2$. The second claim follows by the rows of $\Delta_y^{-1} Q^R$ are mutually distinct with their minimum Euclidean distance being larger than a deterministic sequence $\{\zeta_n\}_{n \geq 1}$. \square

Proof of Lemma 2

By the balanced community sizes assumption and both K_y and K_z are fixed, we have

$$\Delta_y \sum_{l=1}^L B_l \Delta_z^2 B_l^T \Delta_y \preceq c_1 n \Delta_y \sum_{l=1}^L B_l B_l^T \Delta_y \preceq c_1 L n \Delta_y^2 \preceq c_1 L n^2 I_{K_y}, \quad (19)$$

where we used $\Delta_z^2 \preceq \frac{c_0 n}{K_z} I_{K_z}$, $\Delta_y^2 \preceq \frac{c_0 n}{K_y} I_{K_y}$ and $\|\sum_{l=1}^L B_l B_l^T\|_2 \leq L K_y^2$. Recall that the eigen-decomposition of $\Delta_y \sum_{l=1}^L B_l \Delta_z^2 B_l^T \Delta_y$ is $Q^R D^R Q^{R^T}$, (19) implies that D_{ii}^R is upper bounded by $c_1 L n^2$ for any $1 \leq i \leq K$. Note that we use c_1 and c_2 to represent the generic positive constants and they may be different from line to line.

Define $\mathbb{B}^R := \sum_{l=1}^L B_l \Delta_z^2 B_l^T$, by simple calculations, we have

$$\mathbb{B}_{g_i^y g_j^y}^R = \sum_{k_z=1}^{K_z} \sum_{l=1}^L n_{k_z}^z B_{l, g_i^y k_z} B_{l, g_j^y k_z}$$

for all $1 \leq i, j \leq n$. Under the Assumption 1, it is easy to see that

$$\mathbb{B}_{g_i^y g_j^y}^R \geq \frac{n}{c_0 K_z} \left[\sum_{l=1}^L B_l B_l^T \right]_{g_i^y g_j^y}$$

and

$$\mathbb{B}_{g_i^y g_j^y}^R \leq \frac{c_0 n}{K_z} \left[\sum_{l=1}^L B_l B_l^T \right]_{g_i^y g_j^y}.$$

Let $\mu_n^r := c_1 L n^2$, by the decomposition (18), we have

$$\mu_n^r \|U_{i*} - U_{j*}\|_2^2 = \sum_{k=1}^K \mu_n^r \left(\frac{Q_{g_i^y k}^R}{\sqrt{n_{g_i^y}}} - \frac{Q_{g_j^y k}^R}{\sqrt{n_{g_j^y}}} \right)^2$$

$$\begin{aligned}
&\geq \sum_{k=1}^K D_{kk}^R \left(\frac{Q_{g_i^y k}^R}{\sqrt{n_{g_i^y}}} - \frac{Q_{g_j^y k}^R}{\sqrt{n_{g_j^y}}} \right)^2 \\
&= \sum_{k=1}^K D_{kk}^R \left(\frac{Q_{g_i^y k}^R}{\sqrt{n_{g_i^y}}} \right)^2 + \sum_{k=1}^K D_{kk}^R \left(\frac{Q_{g_j^y k}^R}{\sqrt{n_{g_j^y}}} \right)^2 - 2 \sum_{k=1}^K D_{kk}^R \frac{Q_{g_i^y k}^R Q_{g_j^y k}^R}{\sqrt{n_{g_i^y} n_{g_j^y}}} \\
&= \mathbb{B}_{g_i^y g_i^y}^R + \mathbb{B}_{g_j^y g_j^y}^R - 2 \mathbb{B}_{g_i^y g_j^y}^R \\
&\geq \frac{n}{c_0 K_z} \left[\sum_{l=1}^L B_l B_l^T \right]_{g_i^y g_i^y} + \frac{n}{c_0 K_z} \left[\sum_{l=1}^L B_l B_l^T \right]_{g_j^y g_j^y} - 2 \frac{c_0 n}{K_z} \left[\sum_{l=1}^L B_l B_l^T \right]_{g_i^y g_j^y} \\
&\geq c_1 n L \eta_n^r
\end{aligned}$$

for some constant $c_1 > 0$, where the last inequality is implied by our condition, since $\sum_{l=1}^L B_l B_l^T = B^R (B^R)^T$, the $g_i^y g_j^y$ -th element of $\sum_{l=1}^L B_l B_l^T$ is the inner product of $B_{g_i^y}^R$ and $B_{g_j^y}^R$. As a result, for any $Y_{i*} \neq Y_{j*}$, we have $\|U_{i*} - U_{j*}\|_2 \geq c_2 \sqrt{\eta_n^r/n}$ for some constant $c_2 > 0$. \square

Proof of Lemma 3

By the fact that the rank of $\sum_{l=1}^L B_l^T B_l$ is equal to the rank of $\Delta_z \sum_{l=1}^L B_l^T \Delta_y^2 B_l \Delta_z$, we have Q^C is a $K_z \times K$ column orthogonal matrix. It is easy to see that $Z \Delta_z^{-1} Q^C$ has orthogonal columns, so we have

$$V = Z \Delta_z^{-1} Q^C.$$

The rest proof is similar to that of Lemma 1, we omit it here. \square

Proof of Lemma 4

The proof of Lemma 4 follows the same strategy as that of Lemma 2. Here we only describe the difference.

Define $\mu_n^c := c_1 L n^2$ and $\mathbb{B}^C := \sum_{l=1}^L B_l^T \Delta_y^2 B_l$, by simple calculations, we have

$$\mathbb{B}_{g_i^z g_j^z}^C = \sum_{k_y=1}^{K_y} \sum_{l=1}^L n_{k_y}^z B_{l, k_y g_i^z} B_{l, k_y g_j^z}$$

for all $1 \leq i, j \leq n$. Combining this with Assumption 1 and $V = Z \Delta_z^{-1} Q^C$, we have

$$\mu_n^c \|V_{i*} - V_{j*}\|_2^2 \geq \sum_{k=1}^{K'} D_{kk}^C \left(\frac{Q_{g_i^z k}^C}{\sqrt{n_{g_i^z}}} - \frac{Q_{g_j^z k}^C}{\sqrt{n_{g_j^z}}} \right)^2$$

$$\begin{aligned}
&= \mathbb{B}_{g_i^z g_i^z}^C + \mathbb{B}_{g_j^z g_j^z}^C - 2\mathbb{B}_{g_i^z g_j^z}^C \\
&\geq \frac{n}{c_0 K_y} \left[\sum_{l=1}^L B_l^T B_l \right]_{g_i^z g_i^z} + \frac{n}{c_0 K_y} \left[\sum_{l=1}^L B_l^T B_l \right]_{g_j^z g_j^z} - 2 \frac{c_0 n}{K_y} \left[\sum_{l=1}^L B_l^T B_l \right]_{g_i^z g_j^z} \\
&\geq c_1 n L \eta_n^c
\end{aligned}$$

for some constant $c_1 > 0$, where the last inequality is implied by our condition, since $\sum_{l=1}^L B_l^T B_l = B^C (B^C)^T$, the $g_i^z g_j^z$ -th element of $\sum_{l=1}^L B_l^T B_l$ is the inner product of $B_{g_i^z}^C$ and $B_{g_j^z}^C$. As a result, for any $Z_{i*} \neq Z_{j*}$, we have $\|V_{i*} - V_{j*}\|_2 \geq c_2 \sqrt{\eta_n^c/n}$ for some constant $c_2 > 0$. \square

C Auxiliary lemmas

Given a random variable X , we say that Bernstein's condition with parameters v and b holds if $\mathbb{E}[|X|^k] \leq \frac{v}{2} k! b^{k-2}$ for all integers $k \geq 2$. It is also said that X is (v, b) -Bernstein.

Lemma 6 (Theorem 3 in [Lei and Lin \(2022\)](#)). *For $1 \leq l \leq L$, let W_l be a sequence of independent $n \times n$ matrices with zero mean independent entries, and H_l be any sequence of $n \times n$ non-random matrices. If for all $1 \leq l \leq L$ and $1 \leq i, j \leq n$, each entry $W_{l,ij}$ is (v, b) -Bernstein, then for all $t > 0$,*

$$\mathbb{P} \left(\left\| \sum_{l=1}^L W_l H_l \right\|_2 \geq t \right) \leq 4n \exp \left(- \frac{t^2/2}{v \max(n \left\| \sum_{l=1}^L H_l^T H_l \right\|_2, \sum_{l=1}^L \|H_l\|_F^2) + b \max_l \|H_l\|_{2,\infty} t} \right).$$

Lemma 7 (Lemma 5.3 in [Lei and Rinaldo \(2015\)](#)). *Let U be an $n \times d$ matrix with K distinct rows with minimum pairwise Euclidean norm separation $\gamma > 0$. Let \hat{U} be another $n \times d$ matrix and $(\hat{\Theta}, \hat{X})$ be an solution to k -means problem with input \hat{U} , then the number of errors in $\hat{\Theta}$ as an estimate of the row clusters of U is no larger than $c \|\hat{U} - U\|_F^2 \gamma^{-2}$ for some constant $c > 0$.*

Lemma 8 (Theorem 1 in [de la Peña and Montgomery-Smith \(1995\)](#)). *Let $\{X_i\}_{i=1}^n$ be a sequence of independent random variables in a measurable space $(\mathcal{S}, \mathcal{S})$, and let $\{X_i^{(j)}\}$, $j = 1, \dots, k$ be k independent copies of $\{X_i\}$. Let $f_{i_1 i_2 \dots i_k}$ be families of functions of k variables taking $(\mathcal{S} \times \dots \mathcal{S})$ into a Banach space $(\mathcal{B}, \|\cdot\|)$. Then, for all $n \geq k \geq 2$, $t > 0$,*

there exist numerical constant $c_k > 0$ depending on k only so that,

$$\begin{aligned} & \mathbb{P}(\| \sum_{1 \leq i_1 \neq i_2 \neq \dots \neq i_k \leq n} f_{i_1 i_2 \dots i_k}(X_{i_1}^{(1)}, X_{i_2}^{(1)}, \dots, X_{i_k}^{(1)}) \| \geq t) \\ & \leq c_k \mathbb{P}(c_k \| \sum_{1 \leq i_1 \neq i_2 \neq \dots \neq i_k \leq n} f_{i_1 i_2 \dots i_k}(X_{i_1}^{(1)}, X_{i_2}^{(2)}, \dots, X_{i_k}^{(k)}) \| \geq t). \end{aligned}$$

References

- Arroyo, J., A. Athreya, J. Cape, G. Chen, C. E. Priebe, and J. T. Vogelstein (2021). Inference for multiple heterogeneous networks with a common invariant subspace. *Journal of Machine Learning Research* 22(142), 1–49.
- Bakken, T. E., J. A. Miller, S.-L. Ding, S. M. Sunkin, K. A. Smith, L. Ng, A. Szafer, R. A. Dalley, J. J. Royall, T. Lemon, et al. (2016). A comprehensive transcriptional map of primate brain development. *Nature* 535(7612), 367–375.
- Bhatia, R. (1997). *Matrix analysis*, Volume 169 of *Graduate Texts in Mathematics*. Springer-Verlag, New York.
- Bhattacharyya, S. and S. Chatterjee (2018). Spectral clustering for multiple sparse networks: I. *arXiv preprint arXiv:1805.10594*.
- Boccaletti, S., G. Bianconi, R. Criado, C. I. Del Genio, J. Gómez-Gardenes, M. Romance, I. Sendina-Nadal, Z. Wang, and M. Zanin (2014). The structure and dynamics of multilayer networks. *Physics Reports* 544(1), 1–122.
- Chen, S., S. Liu, and Z. Ma (2022). Global and individualized community detection in inhomogeneous multilayer networks. *The Annals of Statistics* 50(5), 2664–2693.
- De Domenico, M., V. Nicosia, A. Arenas, and V. Latora (2015). Structural reducibility of multilayer networks. *Nature Communications* 6, 6864.
- de la Peña, V. H. and S. J. Montgomery-Smith (1995). Decoupling inequalities for the tail probabilities of multivariate u-statistics. *The Annals of Probability* 23(2), 806–816.

- Della Rossa, F., L. Pecora, K. Blaha, A. Shirin, I. Klickstein, and F. Sorrentino (2020). Symmetries and cluster synchronization in multilayer networks. *Nature Communications* 11, 3179.
- Fishkind, D. E., D. L. Sussman, M. Tang, J. T. Vogelstein, and C. E. Priebe (2013). Consistent adjacency-spectral partitioning for the stochastic block model when the model parameters are unknown. *SIAM Journal on Matrix Analysis and Applications* 34(1), 23–39.
- Golub, G. H. and C. F. Van Loan (2013). *Matrix computations*. JHU press, Baltimore.
- Guo, X., Y. Qiu, H. Zhang, and X. Chang (2020). Randomized spectral co-clustering for large-scale directed networks. *arXiv preprint arXiv:2004.12164*.
- Han, Q., K. Xu, and E. Airolidi (2015). Consistent estimation of dynamic and multi-layer block models. In *International Conference on Machine Learning*, pp. 1511–1520. PMLR.
- Holland, P. W., K. B. Laskey, and S. Leinhardt (1983). Stochastic blockmodels: First steps. *Social Networks* 5(2), 109–137.
- Holme, P. and J. Saramäki (2012). Temporal networks. *Physics Reports* 519(3), 97–125.
- Huang, S., H. Weng, and Y. Feng (2022). Spectral clustering via adaptive layer aggregation for multi-layer networks. *Journal of Computational and Graphical Statistics*, 1–15.
- Jing, B.-Y., T. Li, Z. Lyu, and D. Xia (2021). Community detection on mixture multilayer networks via regularized tensor decomposition. *The Annals of Statistics* 49(6), 3181–3205.
- Kivelä, M., A. Arenas, M. Barthélemy, J. P. Gleeson, Y. Moreno, and M. A. Porter (2014). Multilayer networks. *Journal of Complex Networks* 2(3), 203–271.
- Lei, J., K. Chen, and B. Lynch (2020). Consistent community detection in multi-layer network data. *Biometrika* 107(1), 61–73.
- Lei, J. and K. Z. Lin (2022). Bias-adjusted spectral clustering in multi-layer stochastic block models. *Journal of the American Statistical Association*, 1–13.

- Lei, J. and A. Rinaldo (2015). Consistency of spectral clustering in stochastic block models. *The Annals of Statistics* 43(1), 215–237.
- Ma, S., L. Su, and Y. Zhang (2022). Determining the number of communities in degree-corrected stochastic block models. *Journal of Machine Learning Research* 22(310), 1–61.
- MacDonald, P. W., E. Levina, and J. Zhu (2022). Latent space models for multiplex networks with shared structure. *Biometrika* 109(3), 683–706.
- Malliaros, F. D. and M. Vazirgiannis (2013). Clustering and community detection in directed networks: A survey. *Physics Reports* 533(4), 95–142.
- Mucha, P. J., T. Richardson, K. Macon, M. A. Porter, and J.-P. Onnela (2010). Community structure in time-dependent, multiscale, and multiplex networks. *Science* 328(5980), 876–878.
- Noroozi, M. and M. Pensky (2022). Sparse subspace clustering in diverse multiplex network model. *arXiv preprint arXiv:2206.07602*.
- Paul, S. and Y. Chen (2016). Consistent community detection in multi-relational data through restricted multi-layer stochastic blockmodel. *Electronic Journal of Statistics* 10(2), 3807–3870.
- Paul, S. and Y. Chen (2020). Spectral and matrix factorization methods for consistent community detection in multi-layer networks. *The Annals of Statistics* 48(1), 230–250.
- Pensky, M. and T. Zhang (2019). Spectral clustering in the dynamic stochastic block model. *Electronic Journal of Statistics* 13(1), 678–709.
- Rohe, K., T. Qin, and B. Yu (2016). Co-clustering directed graphs to discover asymmetries and directional communities. *Proceedings of the National Academy of Sciences* 113(45), 12679–12684.
- Valles-Catala, T., F. A. Massucci, R. Guimera, and M. Sales-Pardo (2016). Multilayer stochastic block models reveal the multilayer structure of complex networks. *Physical Review X* 6(1), 011036.

- Vu, V. Q. and J. Lei (2013). Minimax sparse principal subspace estimation in high dimensions. *The Annals of Statistics* *41*(6), 2905–2947.
- Zhang, J. and J. Cao (2017). Finding common modules in a time-varying network with application to the drosophila melanogaster gene regulation network. *Journal of the American Statistical Association* *112*(519), 994–1008.
- Zhang, J., X. He, and J. Wang (2022). Directed community detection with network embedding. *Journal of the American Statistical Association* *117*(540), 1809–1819.